Life Science Informatics Publications

Research Journal of Life Sciences, Bioinformatics, Pharmaceutical and Chemical Sciences

Journal Home page http://www.rjlbpcs.com/

RJLBPCS

ISSN 2454-6348

Original Research Article **DOI:10.26479/2019.0501.62**

ADSORPTION AND ANTIBACTERIAL STUDIES USING ENCAPSULATED CHITOSAN/ZnO NANOCOMPOSITE

Muthiah Sakthi Bagavathy, Murugan Perachiselvi, Thambiraj Arthi Feiona, Pitchumani Krishnaveni, E. Pushpalaksmi, V. Swetha, S.John Britto, G. Annadurai*

Division of Nanoscience, Sri Paramakalyani Centre for Excellence in Environmental sciences, Manonmaniam Sundaranar University, Alwarkurichi, India.

ABSTRACT: In this article, Synthesis, Characterization and dye adsorption properties of biocompatible (Chitosan-Znic oxide Nanocomposite was investigated. Zinc oxide Nanoparticle was encapsulated with Chitosan. Physical characterization of Synthesized CS/ZnO was Performed using Fourier transform infra-red (FT-IR), X-ray diffraction (XRD), Scanning electron microscope (SEM), Dynamic light scattering (DLS), and Fluorescence spectra(FL). Methylene Blue dye was used as model pollutant. The isotherm and Kinetic study of dye adsorption was evaluated. The removal efficiency of MB dye was studied at different parameters such as, Effect of dosages, pH and Temperature. The Kinetic behavior was described in terms of Langmuir and freundlich isotherm model, respectively. The Prepared Nanocomposite is also proved to be excellent antibacterial agent against Gram positive and Gram Negative bacteria. Based on the data of present investigation, this paper suggests that CS/ZnO is an efficient and environment-friendly method to degrade MB.

KEYWORDS: CS-ZnO, Adsorption, Methylene Blue. Equilibrium Studies, Antibacterial activity.

Corresponding Author: Dr. G. Annadurai* Ph.D.

Division of Nanoscience, Sri Paramakalyani Centre for Excellence in Environmental sciences, Manonmaniam Sundaranar University, Alwarkurichi, India. Email Address: gannadurai@gmail.com

1. INTRODUCTION

The treatment and dye containing waste water is one of the most serious environmental Problems faced by the automotive, textiles, paper, printing, leather and related industries [1-2]. one of the main

source of waste water pollution are textile industries. The waste water discharged from the textiles is often containing contaminants with intense colour. There are five main methods used for the treatment of dye-containing effluents: adsorption, oxidation–ozonation, biological treatment, coagulation– flocculation, and membrane process [3, 8]. These are the potential threat to our environment and reported to be toxic, hazardous and carcinogenic [3-4]. In addition some of the organic dyes and their product have mutagenic influence on human beings [5].Therefore eradication of dye from the water bodies becomes environmentally important. To, date several techniques such as, chemical oxidation, coagulation/flocculation [6], membrane filtration [7], biodegradation, adsorption have been developed to remove dye effluents [8-12].Among these methods, adsorption technology has proved to be efficient and environment friendly in treating dye effluents and producing high quality water[13-14]. In recent years, a considerable number of studies have focused on low cost alternative materials for the removal of dyes by adsorption method [15-17]. Various conventional physical and chemical methods used for adsorption are often cost prohibitive, while biosorption method is economic [18]. Recently chitosan has been observed for the high potential of the adsorption of dyes [19].chitosan, β-(1-4) acetyl –D- glucosamine, is a linear biopolymer of glucosamine. It can be produced commercially by chemical deacetylation of chitin, a major component of the exoskeleton of crustaceans such as, crabs, shrimps, prawns and lobster. As a natural polymer it is in abundance and has many properties like, non-toxicity, biodegradability, biocompatibility, with ability of the biological activity and film formation [20-26]. It is used as bioadsorbent to remove cationic and anionic dyes due to the presence of amino and hydroxyl groups, which can serve as active adsorption sites [27]. However, chitosan will be used as an effective structure directing agent for the morphology of as-synthesized nanostructure. The goal of Nanotechnology is to make Nanostructure with special properties, which do not exist in their single particle types. Oxide nanoparticles can present unique physical and chemical properties, because of their limited size and high density in their corner or edge surface sites [28-29]. Most of these dyes used by industries are of synthetic origin and are usually stable and difficult to remove by conventional water treatment processes, for example, flocculation, coagulation, chemical precipitation, membrane separation, chemical and biological oxidation, phyto-extraction, ion-exchange, and so forth. Adsorption in this context has been established as the most efficient, ecofriendly, simple, flexible, and cost-effective technique for the treatment of dye-bearing wastewater. In recent years, chitosan based different metal composites such as, chitosan/TiO_2, chitosan/cuprous oxide were prepared increasingly and used as an alternative adsorbent in water

treatment. The aim of this study was to prepare and explore the potential of a promising nano-adsorbent material namely chitosan/Znic oxide metal nanocomposite because both CS/ZnO have good biocompatibility and have been wieldy used in many applications such as biosensor [30] packaging materials [31-32] and drug release carriers [33]. In Earlier reports Laila.Al etal[2017],Arafat.A etal[2015], Anandhavelu etal[2017] synthesized CS-ZnO hybrid composite using Bulk chitosan at pH 6.This paper deals with novel synthesis of biocompatible chitosan/Znic oxide Nanocomposite via insitu chemical precipitation method with Nanochitosan using TPP as a cross linking agent at pH 10 which helps to improve its chemical stability and also its mechanical strength is improved through physical modification which include impregnation of its powder on a support is one of the major advantage of this current studies. However, chitosan-zno nanocomposite is expensive and, accordingly, it is necessary to search for Cheap, easily preparation and efficient sorbents. Chitosan from Prawn waste has attracted great research interest as it offers various advantages such as abundantly available and ability to adsorption and cosmetic application [12]. These sorbents can be disposed of without regeneration because their low cost [13, 14]. Many studies were directed to derive of sorbents from chitosan from Prawn waste and using them in the sorption process was investigated by many studies [15, 16]. The sorption process is depended on the functional groups such as alcohols, aldehydes, lignin, cellulose, ketones, carboxylic, phenolic and ether groups available on the sorbents. Physical characterization of CS/ZnO was performed. Therefore, a suitable, inexpensive Nano-composite material having multiple functionalities could be developed for sustainable multipurpose applications by manipulating their physical forms and/or chemical functionalities. A typical model pollutant (methylene blue dye) was selected to evaluate the adsorption properties of CS/ZnO by batch adsorption experiments. The effect of various experimental parameters on adsorption, such as initial dye concentration, dosage, pH Temperature was studied in detail. In addition the adsorption isotherms and kinetics parameters was investigated.

2. MATERIALS AND METHODS

Chitosan (degree of deactelyation85.0wt %) was purchased from Sigma Aldrich. Znic Acetate dihydrate, Sodium Hydroxide (NaOH), TPP (Tri Poly Phosphate) and Acetic acid were of analytical grade. Methylene blue as adsorbate was obtained from Aldrich chemicals. Deionized water was used throughout the experiments for solution preparations.

2.2 Preparation of Chitosan Solution

1 gram of chitosan was weighed out and dissolved in 100ml of 1% Acetic acid solution and stirrerd at room temperature for about 30min until a clear sol formation. After that the pH of of the solution

was maintained at 6 by adding NaOH and stirred for 30min. Finally 0.5g of TPP was added to above solution with vigorous stirring for 2hours. Then obtained Nano chitosan Particle was centrifuged at 5000rpm for 20min and settled nano chitosan was collected, freeze dried for 24hrs and it was dried at 60^0C in oven for further use.

2.3 Synthesis of Chitosan Based Zinc Oxide Nanocomposite

Preparation of chitosan/Zinc oxide nanocomposite material was carried out by chemical precipitation method using Zinc acetate as a precursor. 0.01M Zinc acetate and 0.05M NaOH was mixed with vigorous stirring for 20 min. During stirring a white precipitate was formed it was collected and filtered with whatman filter paper then dried at room temperature for 2 days. After drying the collected powdered sample was calcinated at 430° C for 30 minutes. After calcination the ZnO Nanoparticle was dispersed in chitosan solution and stirred for 30 min to produce clear solution. Then the pH was adjusted to 10 by adding NaOH. Finally a White product Chitosan/ZnO was washed with deionzed water for several times, and dried in Vacuum at different Temperatures.

2.4 Physicochemical Characterization of CS/ZnO Nanocomposite

FT-IR analysis of the CS/ZnO nanocomposite was performed in (Perkin-Elmer Spectrophotometer Spectrum One) using the transmittance method with wavelength in the range between 450 and 4000$cm^{-}1$ at a resolution of 4 $cm^{-}1$. An XRD spectrum was recorded on a Phillips PW 1800 diffractometer with Cu Kα radiation generated at 40KV for crystalline phase identification. The relative intensity was recorded in the scattering range of 2Ɵ from 10^0 to 80^0. The morphological structure of CS/ZnO sample was examined by scanning electron microscopy (SEM) with a SEM TESCAN (model WEGA11), operating at an accelerating voltage of 25.0KV. Particle size of synthesized Nanocomposite was obtained by Dynamic Light Scattering analysis using (Nanoplus Micromeritics, USA). Perkin Elmer LS45 Fluorescence Spectrometer was used for FL spectroscopic measurements.

2.5 Preparation of Stock Dye Solution

The stock solution was prepared by dissolving 0.5g of dye in 500ml of distilled water. Every experiment was performed at room temperature under a constant agitation speed of 100rpm. The percentage of dye concentration was calculated from the absorbance value before and after the treatment at 664 nm with UV Visible spectrophotometer.

2.6 Batch Adsorption Procedure

The adsorption of MB (Methylene blue) was carried out using batch mode method with effect of different parameters, such as adsorbent dosage (0.1-0.3g/L), solution pH (5.4-7.4) and temperature

(30-60^{0}C) was assessed. Adsorption experiment was performed by adding a desired amount of adsorbent (CS/ZnO) to a conical flask containing 100ml solution of MB (20ppm). Then the sample was placed in a shaker for 24hrs at agitation speed of 100rpm in room temperature. The pH of the MB solution was adjusted by 0.01M HCl and/or 0.1N NaOH before adding the adsorbent. Finally the result was verified with adsorption isotherms and kinetics.

The adsorbed amount dye adsorbed of MB solution was calculated by following equations,

$$q_e = \frac{Ci - Cf}{m} \times v \quad (1)$$

Where q_e = Adsorbed amount (mg/g); C_i- initial concentration of MB (mg/L);C_f- Final concentration of MB (mg/L); V- Volume of adsorbate; m- Mass of used adsorbent (CS/ZnO composite)

2.7 Adsorption Equilibrium

Table 1: Different liberalized form of Langmuir and Freundlich equations

Isotherm	Linear regression	plot	Parameters
Langmuir	$C_e / q_e = (1/K_L q_m) + (C_e / q_m)$	$C_e \ / \ q_e .vs. C_e$	$K_L = slope \ / \ \text{int}\, ercept,$ $q_m = 1 \ / \ slope$
Freundlich	$Log(C_e) = Log(K_F) + 1 \ / \ nLog(C_e)$	$Log(q_e) .vs. Log(C_e)$	$\text{K}_\text{F} = \text{slope}, 1 \ /$ $\text{n} = 1 \ / \ \text{int ercept}$

3. RESULTS AND DISCUSSION

3.1 Fourier Transforms Infrared (FTIR) Studies

To determine the functional group of CS/ZnO Nanocomposite the FT-IR was employed which is shown in Fig (1). The peak exhibit band at 3365cm^{-1}, is due to strong binding of ZnO to the amide group of polymer (chitosan) molecules. The absorption peak at 2924cm^{-1} is asymmetric stretching of CH_3 chitosan polymer. The absorption band at 1634cm^{-1} corresponds to the bending vibration of $–NH_2$ group. The peak formed at 1381cm^{-1}is due to COO- group in carboxylic acid salt. 1159cm^{-1}and 1113cm^{-1} is the special peak of β (1-4) glycosidic bond in the polysaccharide unit. 1022cm^{-1} peak indicate the stretching vibration of C-O-C in glucose circle which corresponds to CH-OH in cyclic compounds [34]. The peak at 847cm^{-1}and 674cm^{-1} is due to Aromatic C-H bending. A new adsorption peak in the range of 478cm^{-1} was found in the FT-IR spectrum of CS/ZnO Nanocomposite, is because of vibration mode of O-Zn-O groups. The reason is that, hydrogen

bonds formed between chitosan and ZnO [35- 40].

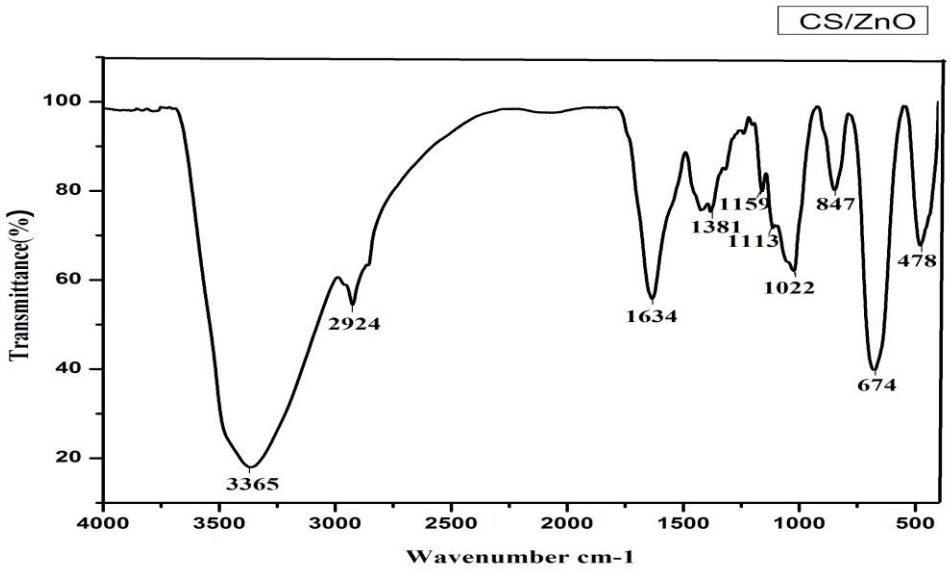

Fig.1. FT-IR Spectra of Encapsulated CS-ZnO Nanocomposite

3.2 X-Ray Diffraction (XRD)

XRD pattern is used to analyze the interlayer changes and crystalline properties of the prepared sample (CS/ZnO) Nanocompoaite. The XRD spectrum of chitosan-Znic oxide Nanocomposite was recorded and the results were stated in Fig (2) which clearly shows the crystalline nature of the material due to sharpness of peaks in the spectra. For pure chitosan, one peak around 2θ value $10^0$and 20^0(41) was proved that chitosan retained a semicrystalline nature in the nanocomposite. Major diffraction peaks was observed at 2θ= 31.9^0, 34.7^0, 37.9^0, 45.6^0, 56.9^0, 63.0^0, 67.9^0, and 75.5^0.This diffraction line was assigned to the (100), (002), (101), (102), (103), (112) and (202) are the crystal planes of pure Znic oxide nanoparticle. These peaks are coherent with the database of Joint Committee on Powder Diffraction standards (JCPDS file, PDF No, (36-1451) [42]. At the same time, the strong diffraction peaks in (100), (002), and (102) are found to be the pattern of CS/ZnO Nanocomposite. According to the Debye Scherrer equation the crystal size of the prepared CS/ZnO Nanocomposite has an average diameter of nm. This result revealed the successful encapsulation on ZnO on chitosan.

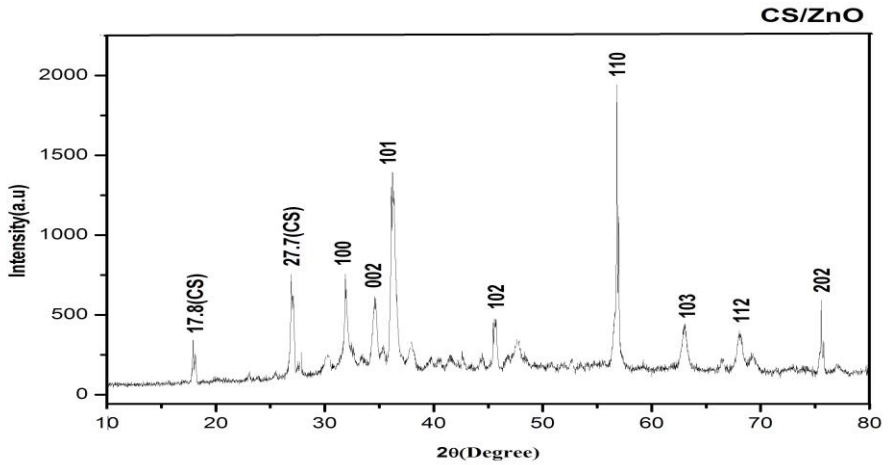

Fig.2. XRD Patters of Encapsulated CS-ZnO Nanocomposite

3.3 SEM (Scanning Electron Microscope) & DLS (Dynamic Light Scattering)

Particle size and surface morphology of the Synthesized Nanocomposite (CS/ZnO) was determined by SEM which shown in Fig (3). As it can be clearly seen that, the CS/ZnO was Polymorphological in shape with aggregation were investigated. Its diameter was found to be 10µm. The average particles size and polydispersity index (PDI) of the synthesized Nanocomposite was determined by DLS and the results was shown in Fig (3). It shows the average particle size of 259.6nm which is well contract with scanning electron microscopy analysis. The Polydispersity index was found to be 0.237 which implies that the synthesized nanocomposites are monodispersed.

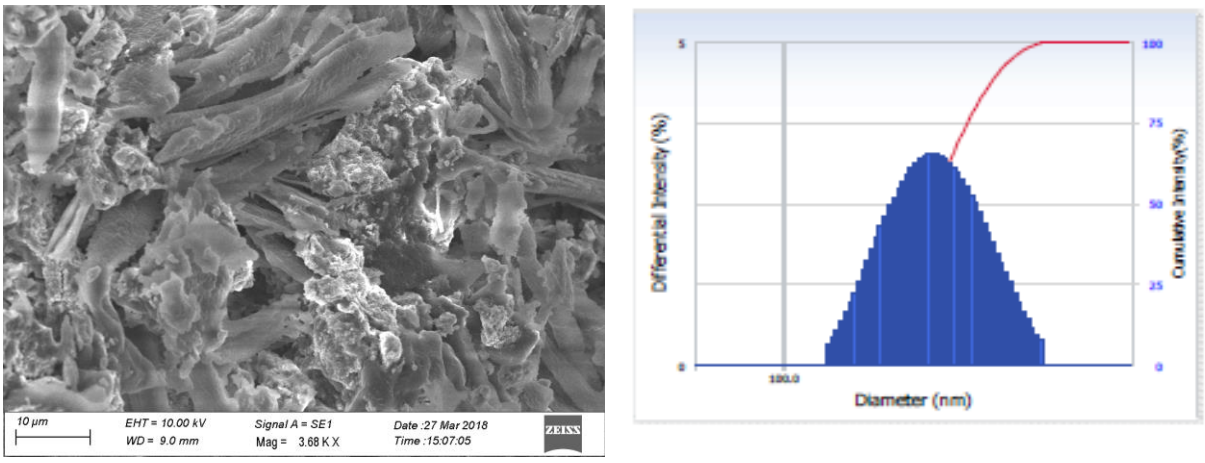

Fig.3. SEM and DLS of Encapsulated CS-ZnO Nanocomposite

3.4 Fluorescence Spectroscopy Analysis (FL)

Fluorescence Spectroscopy Analysis (FL) is used to investigate the band gap of CS/ZnO Nanocomposite. Commonly it also exposed visible emission with a peak in the range from 400-750nm [43]. The visible emission intensity at 409 nm is ascribed to the interstitial oxygen (induced recombination). In the plot, the excitation peaks was observed at 409nm, 645nm and the emission peak at 730nm shown in Fig (4). The most prominent peak in this spectrum was arrayed at 645nm. It represents that encapsulation of chitosan - ZnO Nanocomposites vividly increases the Fluorescence intensity at 645nm is due to change in energy band structure as a result of doping. The excitation peak conform band to band transitions and also affirmed the Red shift in the band-gap of CS/ZnO sample.

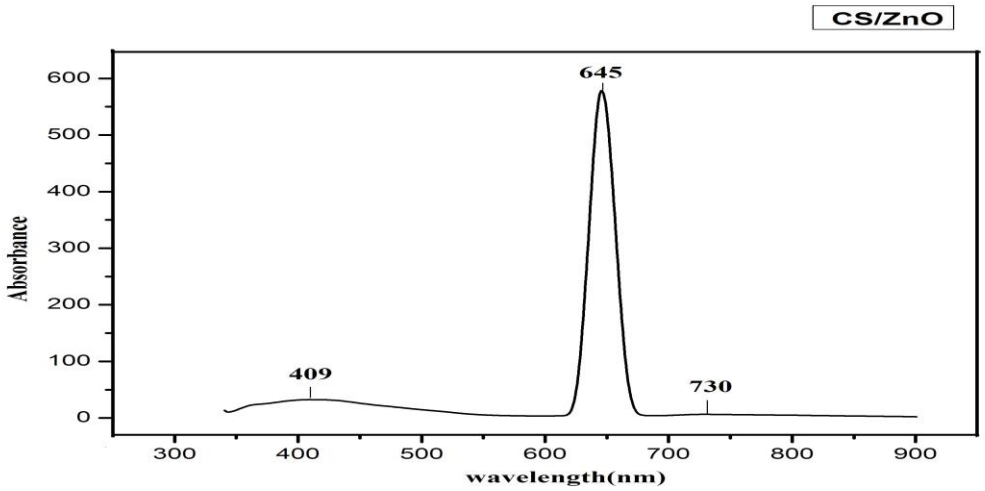

Fig.4. FL Spectra of Encapsulated CS-ZnO Nanocomposite

3.5 Effect Of Adsorbent Dosage

The effect of adsorbent mass on the removal of MB was carried out by varying the dosage of CS/ZnO from 0.1-0.3g/l while keeping other parameters such as, (temperature and pH as constant). The amount of dye removal by adsorbent was represented in Fig (5). It was noticed that the uptake of dye was increased with increasing the adsorbent mass. Almost optimum adsorption was noticed in 0.3g/l of CS/ZnO. Such effect is due to enabling large dye molecule penetrates to all internal pore structure of CS/ZnO Nanocomposite which was reported previously for the adsorption of certain dyes on various adsorbents [Anirudhan etal., 2017; Mohamed etal., 2017; Kashif etal., 2016]. An increase in percentage of removal of MB may be attributed due to increase in adsorbent surface areas, however more active functional groups resulting in the availability of more adsorption sites [44].

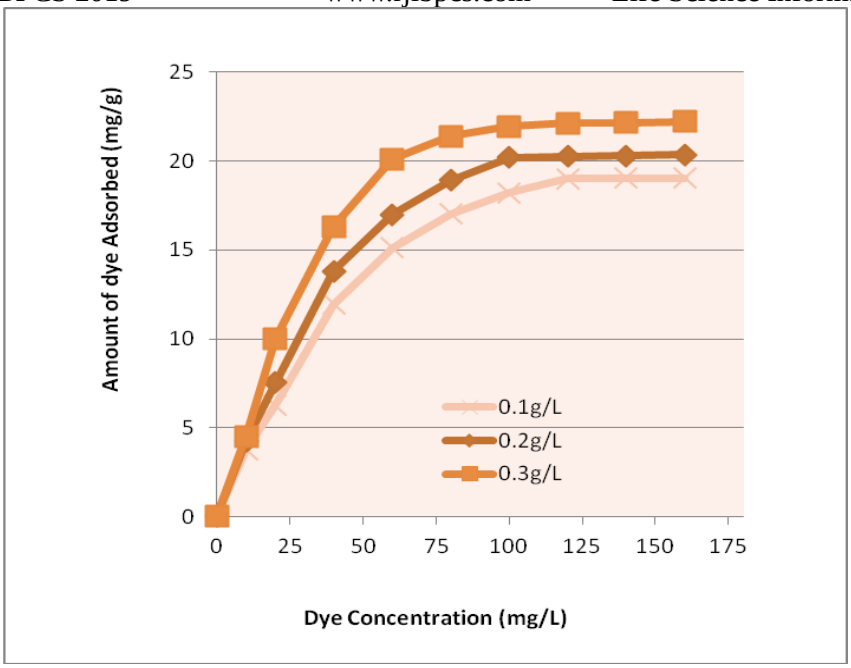

Fig. 5. Maximum Uptake of Methylene blue at different Dosage

3.6 Effect Of PH

The pH is an important parameter in adsorption process because it has the effect on active site of nano-adsorbent and dye speciation during adsorption process [45]. The removal of percentage of MB by CS/ZnO is shown in Fig (6). The pH was maintained in the range of 5.4-7.4 by adding either 0.1M HCL or 0.1MNaOH solution at 0.3g of adsorbent mass by keeping temperature as constant. The highest adsorption was found at pH 6.4, indicating that adsorption was strongly pH dependent. The pH at 6.4 revealed that, all chitosan amino groups are protonated and the repulsion of the polymer chains was carried out at pH lower than 6.5, and the adsorption occurred at the interior of the particles[46].The result showed that the removal MB was increased with increasing pH upto 8 and then decreased. The effect of pH on adsorption was explained by the interaction between the sorbent and sorbate .It mainly affects the surface properties of the sorbent and plays a role onto these surfaces. According to [Yoshida etal., 1997]at lower pH more protons will protonate amine groups of chitosan molecule to form $–NH_2$- Thereby it increases the electrostatic attraction between negatively charged dye anions and positively charged adsorption sites which causes an increase in dye adsorption. This theory agrees with our data on pH effect.

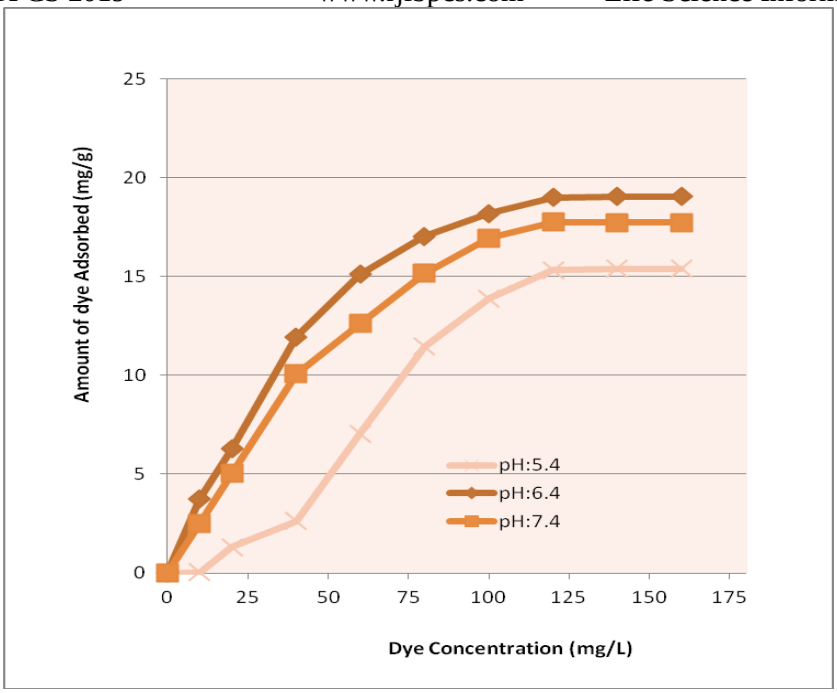

Fig.6. Maximum Uptake of Methylene blue at different pH

3.7 Effect Of Temperature

Temperature is one of the important factors to determine the adsorption. Adsorption isotherm of MB on CS/ZnO was determined at three different temperatures 30^0C, 45^0C and 60^0C which was recorded in Fig (7). It reveals that the amount of MB adsorbed on CS/ZnO increases with increasing concentration non-uniformly and the amount adsorbed increases with increasing temperature implying endothermic process. It may be the result of increase in the mobility of dye with increasing temperature [47]. The endothermic effect was found at above 40^0C. The high temperature favors to the diffusion of dye molecule into the internal porous structure of surface. The curve indicates the strong tendency of monolayer formation [Martina etal., 2017]. Therefore the adsorption capacity strongly depends on chemical interaction between functional groups on adsorbent surface and adsorbate and increases with temperature rising.

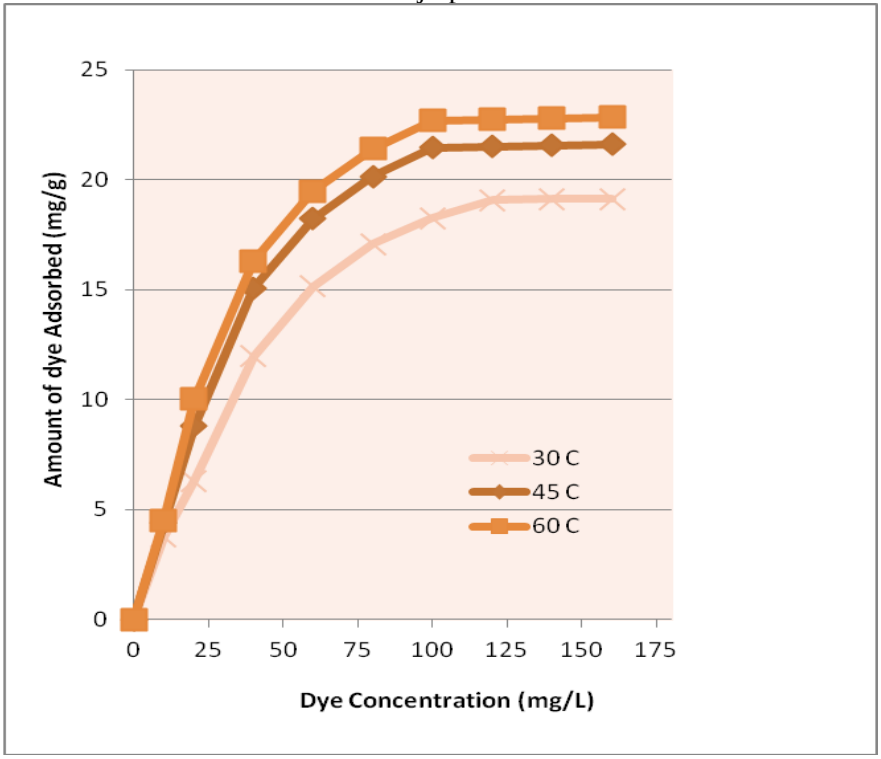

Fig.7. Maximum Uptake of Methylene blue at different Temperature

3.8 Adsorption Isotherms

Adsorption isotherm is an important tool to determine the maximum capacity of adsorption. It also indicates how efficiently the adsorbent will adsorb. To optimize the design of an adsorption system several mathematical models have been used for the adsorption of dyes on adsorbate. In order to adapt for the considered system, one or more isotherm models have been used. In my work, two models was applied namely Langmuir and Freundlich isotherm. The Langmuir isotherm is applicable for homogenous adsorption system whereas Freundlich isotherm is Heterogeneous system.

3.9 Langmuir Isotherm

Equilibrium adsorption isotherm is a basic significance in adsorption frameworks. It communicates connection between mass of colour at specific dose, pH and temperature. A fundamental supposition of the Langmuir hypothesis (Langmuir, 1918) is that the sorption happens at the particular locales inside the adsorbent (Chen et al., 2008; Asfour et al., 1985; Poots et al., 1976). The information gained from the adsorption was fitted in various adsorbent doses, pH and temperature. A plot of ($1/q_e$ versus $1/C_e$) brought about a straight graphical connection demonstrating the appropriateness of the above model as appeared in Fig. 8-10. The Langmuir constant co - efficient accounted on Table 2.

$$q_e = \frac{KbC_e}{(1+bC_e)} \quad (2)$$

$$\frac{1}{q_e} = \frac{1}{K} + \frac{1}{KbC_e} \quad (3)$$

The investigation on measurement of adsorbent is important and valuable to discover the ideal measure of sorbent required for the expulsion of colour. The measure of colour increases in sorbent dose because of accessibility of more surface dynamic locales for the adsorption of methylene blue colour onto the chitosan encapsulated ZnO Nanocomposite. At first, the rate of expulsion of colour is found to increment quickly which hindered as the dosage expanded. The rate of adsorption is higher and more free destinations are accessible and combine the atomic layers increment. From this survey, the measurement of adsorbent at 0.3g/L exposes the maximum removal of methylene blue colour and after increasing the dosage of adsorbent there is no critical change. The pH is an overwhelming parameter in adsorption. The impact of pH in the expulsion of colour was analyzed and the ideal pH for the adsorption of Methylene blue colour onto Chitosan encapsulated Znic Nanocomposite was viable at pH 6.4. The most extreme measure of methylene blue colour by the adsorbents decay at the point, when the temperature was raised from 30 to 60^0C. As the temperature builds, the rate of dispersion of adsorbate atoms over the outer limit layer and interim pores of the adsorbent particles increments. Consequently, the adjustment in the temperature will change the balance limit of the adsorbent for a specific adsorbate.

3.10 Freundlich Isotherm

Freundlich isotherm model stipulates the ratio of solute adsorbed to the solute concentration. It is used for heterogeneous surface system. Show the batch isothermal data fitted to the linear form of the Freundlich isotherm (Dosages, pH, Temperature) as shown in Fig 11-13.

$$q_e = K_F C_e^{1/n} \quad (4)$$

Whereas, (k_f) is sorption capacity; (1/n) is sorption intensity

Various constants associated with isotherm are intercept which indicates the sorption capacity (Kf) and the slope (l/n) sorption intensity were recorded in table (2). Freundlich isotherm is a special case of heterogeneous surface energies. It has been stated by [Sher etal., 2016] that the magnitude of the exponent 1/n gives an indication of the favorability and capacity of the adsorbent/adsorbate system where n>1signifies favorable adsorption conditions. In most of the cases, exponent between 1<n<10 shows beneficial adsorption.

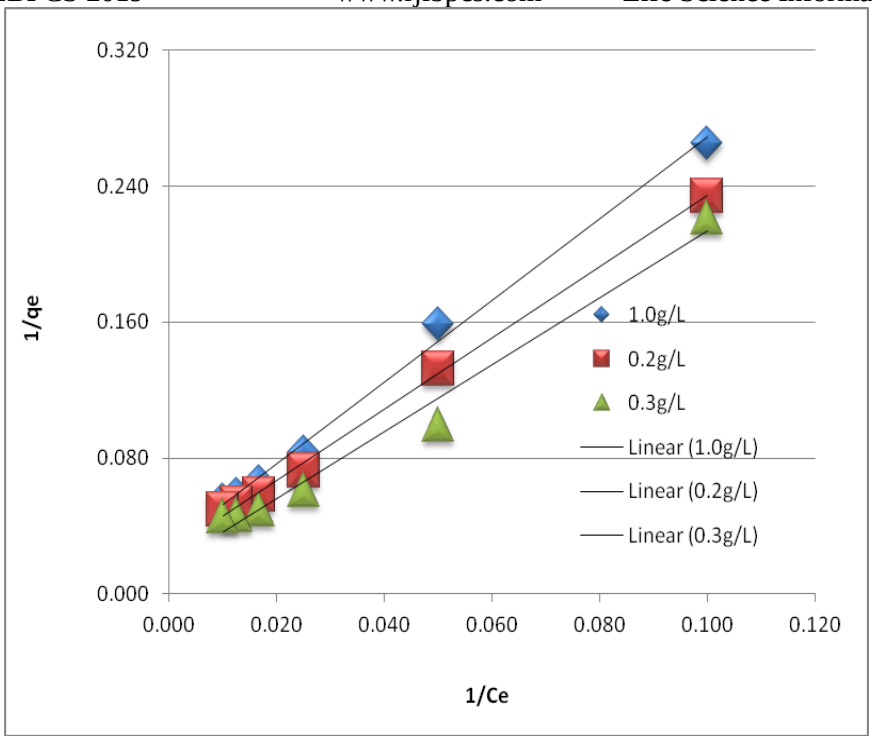

Fig.8. Langmuir isotherm for the removal of Methylene blue using (Encapsulated chitosan-ZnO Nanocomposite) at different dosages

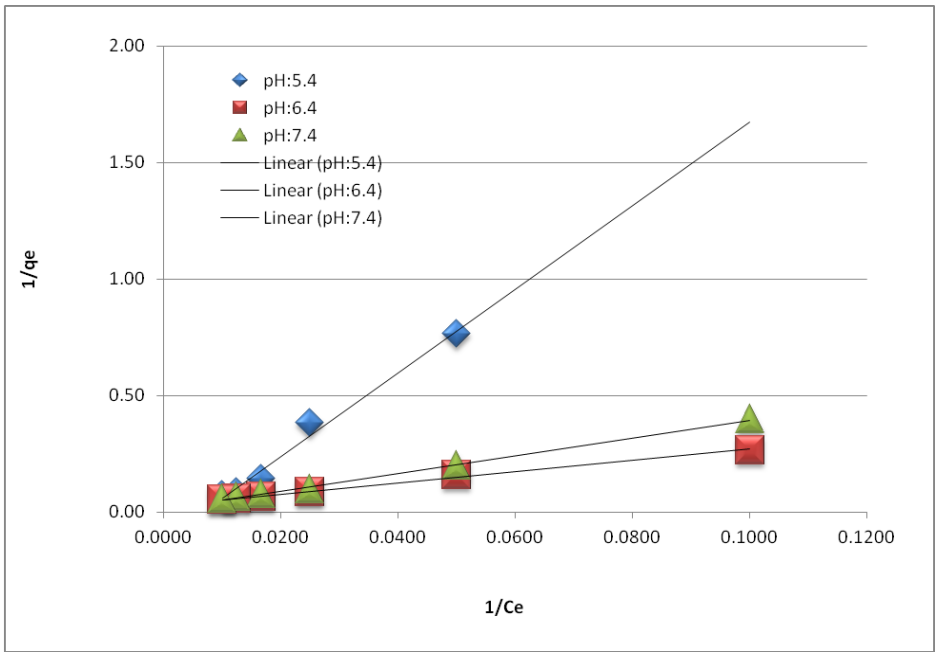

Fig.9. Langmuir isotherm for the removal of Methylene blue using (Encapsulated chitosan-ZnO Nanocomposite) at different pH

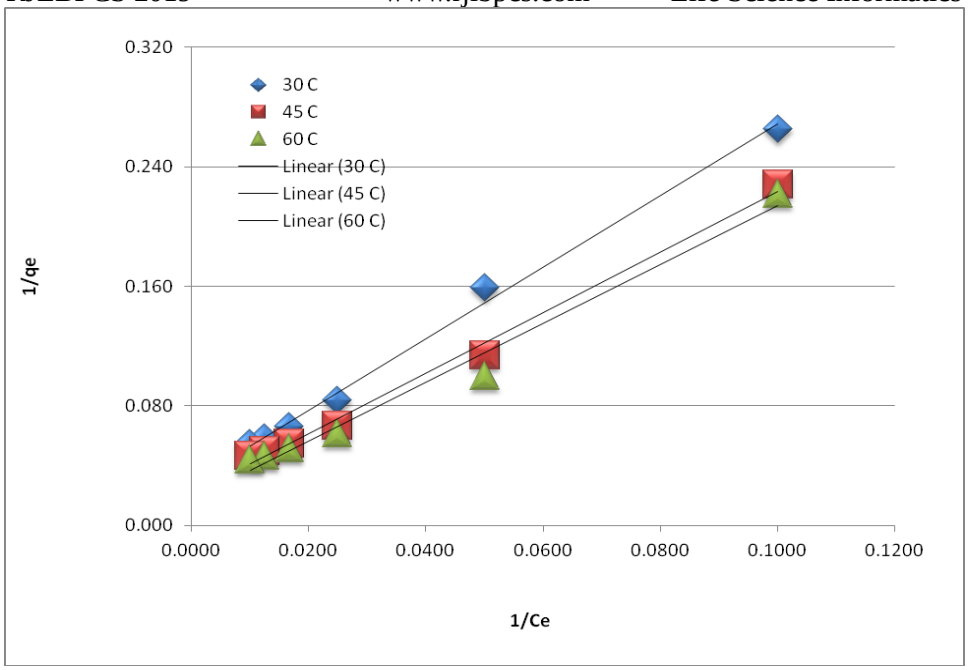

Fig.10. Langmuir isotherm for the removal of Methylene blue using ((Encapsulated chitosan-ZnO Nanocomposite) at different temperatures

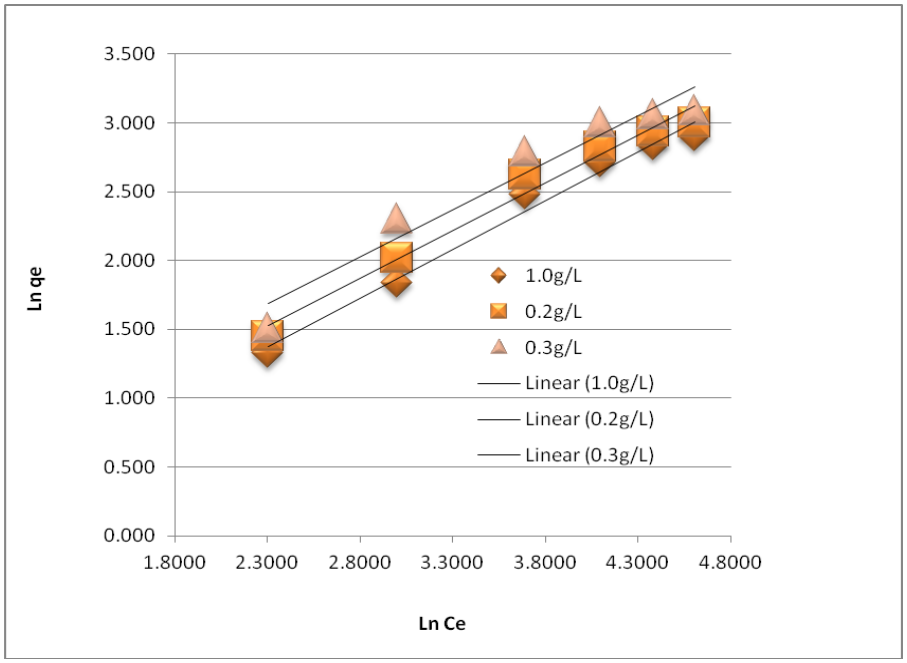

Fig. 11. Freundlich isotherm for the removal Methylene blue using (Encapsulated chitosan-ZnO Nanocomposite) at different adsorbent dosages

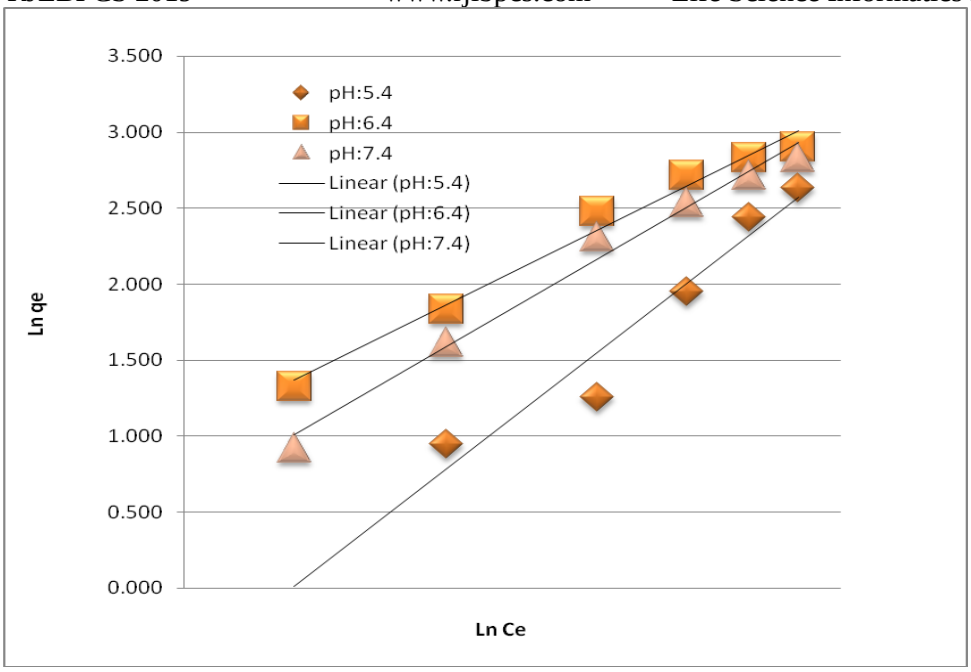

Fig.12. Freundlich isotherm for the removal of Methylene blue using (Encapsulated chitosan-ZnO Nanocomposite) at different pH

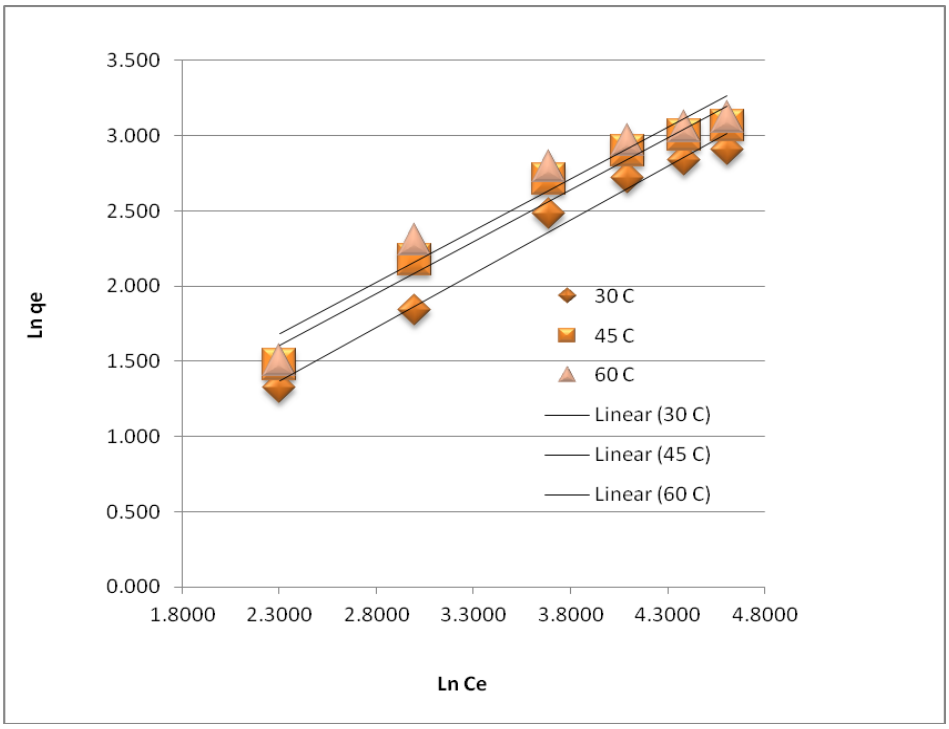

Fig.13. Freundlich isotherm for the removal of Methylene blue using (Encapsulated chitosan-ZnO Nanocomposite) at different temperatures

Table 2: Langmuir and Freundlich isotherm constants at different dosage, temperature and pH (Encapsulated chitosan- ZnO Nanocomposite) – Methylene blue dye

Dosage (g/l)	**Langmuir Isotherm -model parameters**	**Freundlich Isotherm -model parameters**
0.1	K=79.31; b=0.43; R^2= 0.9817	K_F =0.267; n=1.406; R^2=0.89
0.2	K=80.38; b=0.48; R^2= 0.9981	K_F =0.067; n=1.445; R^2=0.86
0.3	K=115.59 ; b=0.51; R^2=0.9956	K_F=0.115; n= 1.466; R^2=0.88
Temperature (^oC)	**Langmuir Isotherm -model parameters**	**Freundlich Isotherm -model parameters**
30	K=82.62; b=0.42; R^2=0.9956	K_F=0.2679; n= 3.73; R^2=0.9829
45	K=96.19; b=0.50; R^2=0.9937	K_F=0.023; n=43.48; R^2=0.9644
60	K=115.88; b=0.51; R^2=0.9826	K_F=0.099; n=10.10; R^2=0.9471
pH	**Langmuir Isotherm -model parameters**	**Freundlich Isotherm -model parameters**
5.4	K=149.61; b=0.06; R^2=0.9859	K_F=0.257; n=3.89; R^2=0.9362
6.4	K=25.20; b=0.26; R^2=0.9976	K_F=0.267; n=3.75; R^2=0.9828
7.4	K=8.00; b=0.42; R^2=0.9956	K_F=0.914; n=1.09; R^2=0.9853

3.11 Antibacterial Activity

Antibacterial activity of synthesized Nanocomposite (CS/ZnO) was tested against gram positive (Bacillus) and gram negative (E-coli) using agar well diffusion method which was exhibited in Fig (13). The zone of inhibition value was shown in Table (3). The inhibitory action towards gram positive pathogen (Bacillus) obtained the value of (4, 2, 2 and 3mm) and gram negative (3.4 and 2mm), for CS/ZnO Nanocomposite. The greater effect was noted in gram positive compared to gram negative bacteria, because gram positive bacteria have one cytoplasmic membrane and the thick cell wall composed of multilayered peptidoglycan whereas gram negative have complex cell wall with peptidoglycan between cytoplasmic membrane and outer membrane. We noticed that CS/ZnO was able to suppress the bacterial growth at lower concentration. The observed results affirmed that the strong anti-biocidal efficiency is due to symbiotic effect of CS/ZnO Nanocomposite [48-49]. Many researchers revealed that CS encapsulated ZnO Nanocomposite had effective antibacterial activity. CS is a cationic polysaccharide, which has positive surface charge and able to attract the negatively charged cell membrane of bacteria whereas ZnO provokes reactive oxygen species which enhance the interaction between CS/ZnO nanocomposites [50-51].

Table 3: Zone of Inhibition of Encapsulated chitosan/ZnO Nanocomposite

Name of Bacteria	100µl µl	120µl	140µl	160µl
Escherichia coli	3mm	4mm	2mm	-
Bacillus sp.	4mm	2mm	2mm	3mm

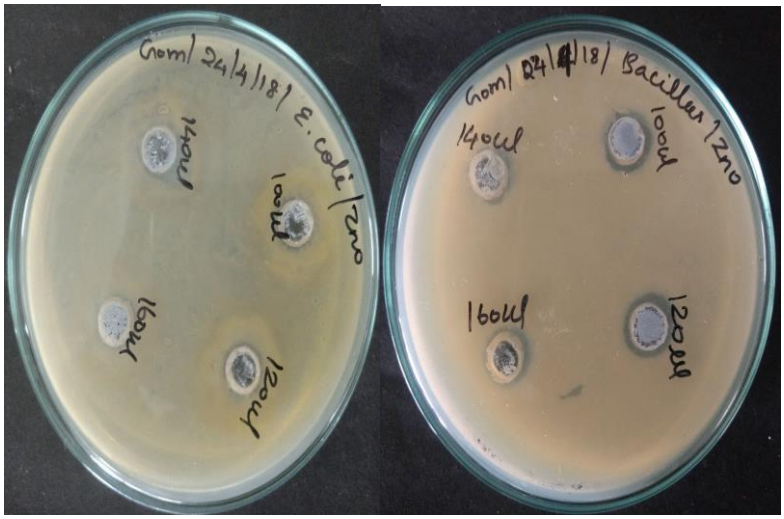

Fig. 13. Antibacterial activity of encapsulated chitosan/ZnO Nano composite

4. CONCLUSION

The study was investigated under invitro condition. CS/ZnO was acted as good adsorbents – adsorption of MB in aqueous solution. Encapsulation of Chitosan-Znic Oxide Nanocomposite was synthesized by chemical precipitation method. CS/ZnO was studied using Fourier Transform infra-red (FT-IR), X-Ray diffraction (XRD), Scanning electron microscopy (SEM), Dynamic light scattering (DLS) and Fluorescence spectroscopy (FL). CS/ZnO has examined under different conditions in batch and equilibrium mode. The equilibrium mode was analyzed using Langmuir and Freundlich isotherms. Furthermore, the antibacterial efficacy of the CS/ZnO was tested against both gram positive and gram negative pathogens using Zone inhibition method. The results revealed that the Synthesized CS/ZnO inhibits the proliferation of bacteria very effectively. In this view of distinguished properties of CS/ZnO Nanocomposite the results suggests that encapsulated chitosan/ZnO Nanocomposite could be used for environmental remediation.

ACKNOWLEDGEMENT

Authors gratefully acknowledge the DST-FIST sponsored programme. Department of science Technology, New Delhi, India for funding the research development (Ref no. S/FST/ESI-101/2010) to carry out this work.

CONFLICT OF INTEREST

Authors have no any conflict of interest.

REFERENCES

1. Fargani H, Lakhmiri R, Albourine A, Cherkaoui O, Safi M. Valorization of shrimp co-products Pandalus borealis": Chitosan production and its use in adsorption of industrial dyes. J. Mater. Environ. Sci. (2016); 7 (4): 1334-1346.
2. Li Y, Chu J, Qi J, Li X. Development of a Gas Sensor Utilizing Chemiluminescence on Nanosized Titanium Dioxide Applied Surface Science. (2001); 257: 6059–6062.
3. Dong XL, Ding W, Zhang XF, Liang XM. Mechanism and kinetics model of degradation of synthetic dyes by UV–vis/H_2O_2/Ferrioxalate complexes. Dyes Pigm. (2007); 74: 470–476.
4. Elwakeel KZ, and Guiba E . Arsenic(V) sorption using chitosan/$Cu(OH)_2$ and chitosan/CuO composite sorbents Carbohydr. Polym. (2015);134: 190–204.
5. Fan C, Luo,X., Li F, Lu H, Qiu M. Sun Fabrication of novel magnetic chitosan grafted with graphene oxide to enhance adsorption properties for methyl blue, Journal of Hazardous Materials. (2012); 216:272–279.
6. Guibal E, and Roussy J. Reactive and Coagulation and flocculation of dye-containing solutions using a biopolymer (Chitosan) Functional Polymers. (2007); 67: 33–42.
7. Capar G , Yetis U, Yilmaz L. Membrane based strategies for the pre-treatment of acid dye bath wastewatersJournal of Hazardous Materials. (2006); 135: 423–430.
8. Pandit.P, and Basu S. Removal of ionic dyes from water by solvent extraction using reverse micelles, Environ. Sci. Technol. (2004); 38: 2435–2442.
9. Li Y.J, Li X.D, Li J.W, Yin J. Photocatalytic degradation of methyl orange by TiO2- coated activated carbon and kinetic study, Water Res. (2006);40: 1119–1126.
10. Alinsa A, Khemis M, Pons MN. Leclerc JP, Yaacoubi A., Benhammou A., Nejmeddine A., Electro-coagulation of reactive textile dyes and textile wastewater. Chem. Eng. Process. (2005); 44: 461–470.
11. Cheng G, Xiong JY, Stadler FJ. A facile polyol-mediated approach to tunable CeO2 microcrystals and their photocatalytic activity. Powder Technol. (2013): 249: 89–94.
12. Deepa. K , Chandran P, Khan S.S. Bioremoval of Direct Red fromaqueous solution by Pseudomonas putida and its adsorption isotherms and kinetics, Ecol. Eng. (2013); 58: 207–213.

13. Zhang WJ, Zhou CJ, Zhou WC, Lei AH, Zhang QL., Wan Q., Zou BS. Fast and considerable adsorption of methylene blue dye onto graphene oxide. Bull. Environ. Contam. Toxicol. (2011); 87: 86–90.
14. Kumar KY, Muralidhara HB, Nayaka YA, Balasubramanyam J, Hanumanthappa H. Low-cost synthesis of metal oxide nanoparticles and their application in adsorption of commercial dye and heavy metal ion in aqueous solution, Powder Technol. (2013); 246: 125–136.
15. Safa, Hand Bhatti N. Kinetic and thermodynamic modeling for the removal of Direct Red-31 and Direct Orange-26 dyes from aqueous solutions by rice husk. Desalination (2011);272: 313–322.
16. Cardoso NF, Lima EC, Calvete T, Pinto IS, Amavisca CV, Fernandes THM, Pinto RB, Alencar WS. Application of Aqai Stalks As Biosorbents for the Removal of the Dyes Reactive Black 5 and Reactive Orange 16 from Aqueous Solution Journal of Chemical Engineering Data. (2011);56: 1857–1868.
17. Deng H, Lu J, Li G, Zhang G, Wang X. Adsorption of methylene blue on adsorbent materials produced from cotton stalk Chemical Engineering Journal. (2011); 172: 326–334.
18. Hamzeh, Y. Ashori, A. Azadeh E, Abdulkhani A. Removal of Acid Orange 7 and Remazol Black 5 reactive dyes from aqueous solutions using a novel biosorbent. Materials Science and Engineering. C. (2012) 32: 1394–1400.
19. Chiou MS, Ho PY, Li HY. Adsorption of anionic dyes in acid solutions using chemically cross-linked Chitosan beads Dyes Pigments. (2004); 60: 69–84.
20. Crini G. Studies on adsorption of dyes on beta-cyclodextrin polymer, Bioresour. Technol. (2003); 90: 193–198.
21. Crini. G. Recent developments in polysaccharide-based materials used as adsorbents in wastewater treatment, Prog. Polym. Sci. (2005); 30: 3870.
22. Crini G.and Badot PM. Application of chitosan, a natural aminopolysaccharide, for dye removal from aqueous solutions by adsorption processes using batch studies: a review of recent literatureProg, Polym. Sci. (2008); 33: 399–447.
23. Hansan S, Krishnaiah A, Ghosh TK, Adsorption of chromium(VI) on chitosan coated perliteSep, Sci. Technol. (2003); 38: 3775–3793.
24. Liu BJ, Wang DF, Xu Y, Huang G., Adsorption properties of Cd(II)-imprinted chitosan resin J, Mater. Sci. (2011); 46: 1535–1541.
25. Muzzarelli RAA, and Muzzarelli C. Polysaccharides 1: Structure, Characterization and Use, In: T.Heinze, (ED), Springer. (2005);151–209.

26. Ozmen EY, Sezgin M, Yilmaz A, Yilmazm M. Synthesis of bcyclodextrin and starch based polymers for sorption of azo dyes from aqueous solutions, Bioresour. Technol. (2008); 99: 526–531.
27. Wu FC, Tseng RL, Juang, RS. Kinetic modeling of liquid-phase adsorption of reactive dyes and metal ions on chitosan Water Research. (2001);35: 613–618.
28. Bhattacharjee CR, Purkayastha DD, Bhattacharjee, S, Nath A. Homogeneous chemical precipitation route to ZnO nanospherical, Assam Univ, J. Sci. Technol: Phys. Sci. Technol. (2011); 7 (2): 122–127
29. Fernandez-Garcı M, and Rodriguez JA. Metal Oxide Nanoparticles, Encyclopedia of Inorganic Chemistry. (2009);18(4):377-382.
30. Zhao M, Huang J, Zhou Y. A single mesoporous ZnO/chitosan hybrid nanostructure for a novel free nanoprobe type biosensor. Biosens. Bioelectron. 2013; 43:226–230.
31. Youssef AM, Abou-Yousef H, El-Sayed SM. Mechanical and antibacterial properties ofnovel high performance chitosan/nanocomposite films. Int. J. Biol. Macromol. 2015; 76: 25–32.
32. Wang Y, Zhang Q, Zhang CL. Characterisation and cooperative antimicrobial propertiesof chitosan/nano-ZnO composite nanofibrous membranes. Food Chem. 2012; 132:419–427
33. Yuan Q, Hein S, Misra RDK. New generation of chitosan-encapsulated ZnO quantum dots loaded with drug: synthesis, characterization and *in vitro* drug delivery response. Acta Biomater. 2010; 6:2732–2739.
34. Kumirska M, Czerwicka Z, Kaczynski A, Bychowska K, Brzozowski J, Thoming P. Stepnowski. Application of spectroscopic methods for structural analysis of chitin and chitosan, Mar. Drugs. (2010); 8: 1567–1636.
35. Andres-Verges M, Serna CJ. Morphological characterization of ZnO powders by X-ray and IR spectroscopy. J. Mater. Sci. Lett. (1988); 7: 970–972.
36. Brugnerotto J, Lizardi J, Goycoolea FM, Arguelles W. - Monal, J. Desbrieres, M. Rinaudo,M An infrared investigation in relation with chitin and chitosan characterization, Polymer.(2001); 42: 3569–3580.
37. Dong ZF, Du YM, Fan LH, Wen Y, Liu H, Wang XH. Preparation and properties of chitosan/gelatin/nano-TiO2 ternary composite films, J. Funct. Polym. (2004); 17: 61–66.
38. Li LH, Deng JC, Deng HR, Liu ZL, Xin L. Synthesis and characterization of chitosan/ZnO nanoparticle composite membranes, Carbohydr. Res. (2010); 345: 994–998.

39. Pearson FG, Marchessault CY, Liang V. Chitin, Infrared spectra of crystalline polysaccharides, J. Polym. Sci. (1960); 43: 101–116.
40. Salehi R, Arami M, Mahmoodi NM, Bahram H. Khorramfar S. Novel biocompatible composite (chitosan zinc oxide nanoparticle): preparation, characterization and dye adsorption properties, Colloids Surf. B. (2010); 80 (1): 86–93.
41. Corbridge D.C and .Lowe .J. The Infra-red Spectra of some inorganic phosphorous compounds, J. Chem. Socpp.(1954); 12: 493-502.
42. Li LH, Deng JC, Deng HR, Liu ZL, Xin L. Synthesis and characterization of chitosan/ZnO nanoparticle composite membranes, Carbohydr. Res. (2010); 345: 994–998.
43. Nyffenegger B, Craft M, Shaaban S, Gorer G, Erley RM, Penner A. Hybrid Electrochemical/Chemical Synthesis of Zinc Oxide Nanoparticles and Optically Intrinsic Thin Films. Chem. Mater. (1998); 10: 1120-1126.
44. MalekbalaHosseini MR, Kazemi Yazdi S, Masoudi Soltani S, Malekbala MR. Recent Developments of Textile Waste Water Treatment by Adsorption Process: A Review. Chemical Engineering Research Design. (2012); 90: 704–712.
45. Arshadi M, Salimi Vahid F, Salvacion JWL, Soleymanzadeh M. A practical organometallic decorated nano-size SiO2–Al2O3 mixed-oxides for methyl orange removal from aqueous solution, Appl. Surf. Sci. (2013);280: 726–736.
46. Crini G, and Badot PM. Application of chitosan, a natural aminopolysaccharide, for dye removal from aqueous solutions by adsorption processes using batch studies: A review of recent literature. Prog. Polym. Sci. (2008); 33: 399–447.
47. Alkan M, and Dogan M, Adsorption kinetics of Victoria blue onto perlite, Fresen. Environ. Bull. (2003); 12: 418–425.
48. Veerapandian M, Lee MH, Krishnamoorthy K., Yun K. Synthesis, Characterization and Electrochemical Properties of Functionalized Graphene Oxide. Carbon. (2012); 50: 4228–4238.
49. Akhavan O,. and Ghaderi, E. Toxicity of Graphene and Graphene Oxide Nanowalls Against Bacteria. ACS Nano. (2010); 4: 5731–5736.
50. Sundar K., Harikarthick V, Karthika VS, Ravindran A. Preparation of Chitosan-Graphene Oxide Nanocomposite and Evaluation of Its Antimicrobial Activity. J. Bionanosci. (2014); 8: 207–212.
51. Gupta J, Bhargava P, Bahadur D. Fluorescent Zno for Imaging and Induction of DNA Fragmentation and Ros-Mediated Apoptosis in Cancer Cells. J. Mater. Chem. B. (2015); 3: 1968–1978.